Available online at www.sciencedirect.com
SCIENCE DIRECT
Polymer 47 (2006) 2519–2525
polymer
www.elsevier.com/locate/polymer

Visualization of degradable worm micelle breakdown in relation to drug release

Yan Geng, Dennis E. Discher *

Department of Chemical and Biomolecular Engineering, University of Pennsylvania, Philadelphia, Pennsylvania, PA 19104-6391, USA

Received 25 August 2005; received in revised form 7 November 2005; accepted 9 November 2005
Available online 7 February 2006

Abstract

Spherical micelles and spherical vesicles have been extensively studied as carriers of hydrophobic drugs, but highly elongated polymer-based worm micelles might also serve the same purpose if release mechanisms are integrated. Degradable amphiphilic copolymers of poly(ethylene oxide)-*block*-polycaprolactone, PEO-*b*-PCL, are labeled here with hydrophobic dye and shown by fluorescence microscopy to assemble into highly flexible worm micelles. Degradation-induced morphological transitions from worms to spheres are quantitated in terms of decreasing contour lengths. The hydrophobic core of PCL can carry hydrophobic drugs in addition to dyes, as illustrated here by loading efficiency, storage, and degradation-coupled release of a model hydrophobic anti-cancer drug, taxol. From this, it can be estimated that single worm micelle about 10 μm long is additionally estimated to carry and release enough taxol to kill a single cell. The transition-coupled release is explained in part by the fact that worms have a larger volume-to-area ratio compared to spheres of the same radius.

Keywords: Polyesters; Taxol; Degradation

1. Introduction

Block copolymer amphiphiles with a hydrophilic block covalently linked to a hydrophobic block are capable of self-assembly analogous to conventional small-molecule surfactants (<1 kDa). Cylindrically shaped worm micelles together with spherical micelles and vesicles define at least three stable morphologies [1]. Provided the hydrophobic block is sufficiently massive to drive assembly and overcome hydrophilic features such as high oxygen content, morphology of self-assemblies is generally dictated by block ratios [2], and desired physicochemical properties can be tuned through molecular weight (M_n), block structure, segment modification and crosslinking [3–7]. Such broad flexibility in design of copolymer macro-surfactants cannot only be realized but can also offer clear material advantages over small surfactants. Moreover, copolymer assemblies can be much more stable systems compared to small surfactants, since they generally have much lower critical micellar concentration (CMC$\sim$exp($-M_n$)) and slower dissociation rate [8]. These features of diblock copolymers make them potentially useful in many applications, in particular as drug delivery vehicles [9].

In the last 20 years, there has been increasing interest in exploration of polymer-based spherical micelle systems as drug delivery vehicles, especially using biocompatible/degradable copolymers [10–15]. Poly(ethylene oxide), PEO, is most commonly used as a hydrophilic block due to its biocompatibility, and polylactide or polycaprolactone are among the most common hydrophobic blocks due to the hydrolytic degradation mechanisms of these polyesters. While the hydrophobic core can load drugs of poor water solubility, the outer hydrophilic corona maximizes biocompatibility and helps micelles escape rapid clearance by the liver and spleen after intravenous administration—prolonging circulation in blood [16,17]. Spherical micelles are proving extremely useful for therapeutic applications: they are able to incorporate drugs, permeate tissues with small pores, provide sustained release of the drug, reduce toxic side-effects, enhance the therapeutic efficiency of the drug, and also provide platforms for targeting [1,18,19].

Worm micelles are beginning to show promise as novel carriers that provide larger core volume (per carrier) for drug loading with an ability to flow readily through capillaries and pores because of their small cross-section as well as flexibility [20,21]. While degradable spherical micelles show little change in shape or size change with degradation, obscuring

* Corresponding author. Tel.: +1 215 898 4809; fax: +1 215 573 6334.
E-mail address: discher@seas.upenn.edu (D.E. Discher).

0032-3861/$ - see front matter © 2006 Elsevier Ltd. All rights reserved.
doi:10.1016/j.polymer.2005.11.093

mechanisms [11–15], hydrolytic degradation drives worm micelles to spontaneously shrink into spherical micelles due to a dominant 'end-cleavage' mechanism that appears kinetically tunable with temperature, pH and M_n of the polymer [23]. Thus, one potentially useful and novel strategy for drug delivery would be to start with worm micelles having a large drug-loading capacity and long circulation time [22] that then progressively degrade into spherical micelles either in the bloodstream or at a target site (e.g. tumor). Degradation should also lead to drug release, but it is not clear whether the drug should release before, during, or after the worm-to-sphere transition.

To clarify release mechanism, we need to better characterize worm-to-sphere transition kinetics. Fluorescence video microscopy (FM) has been widely used to study cellular structures and dynamics of biopolymers, but it has also been proven useful recently for visualizing micron-long worm micelles [20,24]. Beyond the advantages of simple sample preparation and direct visualization in aqueous solutions (rather than frozen or fixed samples required for Electron Microscopy, EM [25]), FM is also done in thick chambers and not in $\sim$100 nm, films needed to constrain for EM. FM thus provides more equilibrated and convenient access to length measures and stability in the absence of squeezing and fragmentation that would seem unavoidable with soft objects in thin films (for EM). Moreover, real-time video of thermodynamic fluctuations of worm micelles could be captured through FM to analyze their flexibility and dynamics.

In this paper, we use FM to visualize giant and flexible worm micelles made from degradable copolymers of poly (ethylene glycol)-*block*-polycaprolactone, PEO-*b*-PCL (denoted OCL), and we quantify morphological changes induced by PCL degradation. We also investigate their biocompatibility with blood and cultured cells, as well as the loading of a clinical hydrophobic drug, taxol [26], which is used to inhibit cancer cell growth in tumors and smooth muscle cell proliferation on stents. We then describe storage conditions and how degradation couples to the release kinetics of taxol from these OCL worm micelles.

2. Experimental

2.1. Materials

Diblock copolymers of poly(ethylene oxide)-*b*-poly (ε-caprolactone), PEO–PCL (denoted OCL), with weight fractions of PEO, $f_{EO}\sim0.42$, of two molecular weights, OCL1 ($M_n=2000$–2770, polydispersity PDI$=M_w/M_n=1.19$) and OCL3 ($M_n=5000$–6500, $M_w/M_n=1.3$) were from Polymerscource, Inc., organic solvent (chloroform), Spectra/Por dialysis tubing, syringe filter, glass slides and coverslips were from Fisher, taxol was from Molecular Probes, Inc., and the fluorescent dye PKH 26 and the standard pH 7 PBS and pH 5 Hepes buffers were from Sigma-Aldrich.

2.2. Preparation of OCL worm micelles by cosolvent/evaporation method

OCL worm micelles were prepared by a cosolvent/evaporation method [23]. Briefly, 1 mg of the OCL film was dissolved in 30 μl chloroform, and 5 ml of water was added and stirred for 1–2 h, yielding an opaque worm micelle dispersion. Chloroform ($\sim$0.5% of solution volume) was then removed by evaporation at 4 °C to minimize OCL worm micelle degradation. The final OCL worm micelle solution (0.2 mg/ml) exceeds the CMC [27] of OCL copolymers <1.2 μg/ml by a factor 100, and thus OCL copolymers are mainly in the form of micelles in aqueous solutions.

2.3. Fluorescence microscopy (FM) of OCL worm micelle morphology and thermodynamics

A hydrophobic fluorescent dye (PKH 26) was added to the OCL worm micelle aqueous solutions in order to visualize the assemblies in a chamber formed between glass slide and coverslip. OCL worm micelles were imaged with an Olympus IX71 inverted fluorescence microscope using a 60× objective and a Cascade CCD camera. Two microliters of sample was used in the chamber and approximately 20 pictures were taken per sample [24].

2.4. Cell culture

Bovine aortic endothelial cells and vascular smooth muscle cells were purchased from ATCC (American Type Culture Collection). Cells were plated and allowed to attach for 12 h, after which a measured dose of OCL worm micelles in PBS was added to each plate. Cell viability after exposure to OCL worm micelles for up to 5 days was assayed by Trypan Blue exclusion.

2.5. Hemolysis study

Fresh whole blood was pelleted by centrifugation and 100 μl of the collected red blood cell (RBC) suspension was added to 900 μl of 10 mg/ml OCL worm micelles in PBS (RBC: 10% hematocrit in PBS). The samples were incubated for 24 h at 37 °C. The release of hemoglobin in the supernatant, collected by centrifugation, was measured by UV–vis at 412 nm and compared to the complete hemolysis by 0.2% small surfactants Triton X-100.

2.6. Taxol loading

Stock solutions of taxol (Paclitaxel: tax-11-en-9-one, 5β, 20-epoxy-1,2α,4,7β,10β,13α-hexahydroxy-4,10-diacetate-2-benzoate-13-(α-phenylhip-purate) in methanol (5 mg/ml) was added with a weight ratio of 0.2:1 to 1 ml of OCL worm micellar solutions at different concentrations (0.1, 0.5, 1 wt%), and vortexed for 5 min. The small amount of methanol was removed by dialysis at 4 °C for 2 h. Unloaded free taxol precipitate was centrifuged down at 3000 rpm for 5 min and

further removed from the micelle supernatant by filtering with a 0.45 μm pore-sized syringe filter [28,29]. The amount of taxol loaded into OCL worm micelles was then determined by HPLC. A Waters Breeze HPLC equipped with a diode array UV detector set at $\lambda = 220$ nm, connected with a Symmetry C-18 column, methanol as the mobile phase, and a flow rate of 0.8 ml/min was used. Before injecting into HPLC, taxol loaded OCL worm micelles was lyophilized and redissolved in methanol and filtered with a 0.45 μm syringe filter. Taxol is well resolved from OCL peak, and the amount of taxol was estimated from its calibration curve that correlates its peak area with amount.

2.7. Taxol release

The release behavior of taxol from OCL worm micelles under different pH buffers (0.01 M PBS pH 7 and 0.01 M HEPES pH 5) was studied by dialysis at 37 °C. Ten millilitres of taxol encapsulated 0.2 mg/ml OCL worm micelle buffered solution was put into a dialysis tubing (MWCO: 1000). The dialysis bag was then placed in a 1 liter beaker filled with the same 0.01 M buffer aqueous solutions. At the specific time intervals, a 150 μl aliquot was removed from the dialysis bag, lyophilized and re-dissolved in $CHCl_3$. Buffer salt was centrifuged down at 3000 rpm for 5 min and further removed from the micelle supernatant by filtering with a 0.45 μm pore-sized syringe filter. $CHCl_3$ was then evaporated under the stream of N2 and the mixture of taxol and OCL polymer was redissolved in 150 μl methanol and filtered through a 0.45 μm pore-sized syringe filter before injecting into HPLC. The amount of taxol remaining in the dialysis bag was estimated from its calibration curve and the percentage of released taxol was calculated as %-Release = (total taxol − taxol remained in dialysis bag)/total taxol × 100%.

3. Results and discussion

3.1. Visualization and characterization of degradable OCL worm micelles

Giant and flexible worm micelles were self-assembled from amphiphilic, degradable copolymer PEO–PCL (OCL). Both copolymers studied have a PEO weight fraction of $f_{EO} \sim 0.42$, which favors worm micelle formation [2], but they have different molecular weights OCL1: $M_n \sim 4700$ and OCL3: $M_n \sim 11{,}000$, which should influence worm micelle physical properties and also drug loading, we hypothesized. Before studying the latter, the worm micelles were labeled with the hydrophobic fluorescent dye PKH26 and then imaged fluorescence video microscopy (FM). The contour of the OCL worm is well resolved (Fig. 1a) and considerably exceeds the optical resolution of the microscope (~250 nm). Sequential snap-shots show the thermal fluctuations of a single worm micelle (Fig. 1a) and thus demonstrate the flexibility of these giant micelles. Overlays of skeletonized contours show that the distance R between worm ends fluctuates considerably, allowing an evaluation of the thermal average

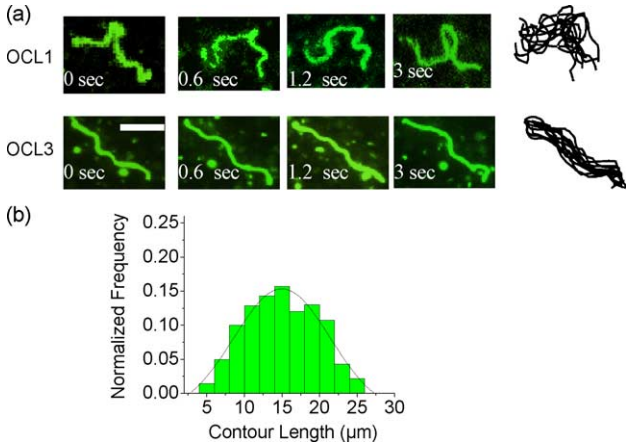

Fig. 1. Visualization and thermo-dynamics of worm micelles self-assembled from OCL copolymer by fluorescence microscopy (FM). (a). Dynamic snapshots and overlay of 10 backbone traces of a single OCL worm micelle. Scale bar is 10 μm. (b). Contour length distribution measured by FM and fit by a Gaussian (for 200 worms).

$\langle R^2 \rangle = 2l_p^2[L/l_p - 1 + \exp(-L/l_p)]$ in terms of the measured contour length L of the worm and the flexibility of the worm as a persistence length, l_p [20,24]. From the analysis of many worm micelles (>100 worms), we determine an average $l_p = 500 \pm 200$ nm for OCL1, and 5 ± 2 μm for OCL3 worm micelles, respectively.

Both the persistence length l_p and diameter d of OCL worm micelles ($d \approx 11$ nm for OCL1 and 29 nm for OCL3 as measured by TEM [7], Suppl. Fig. 1) are essentially the same as those of worm micelles made from non-degradable PEO–PBD with similar M_n. All of the worm micelle systems fit well to the scaling relation $l_p \sim d^{2.8}$ that is indicative of a fluid rather than a glassy aggregate [30]. We use the physical methods and considerations above to assess below the possible effects of taxol loading on worm micelle physical properties. For example, any significant swelling of the core would increase d and influence l_p. Likewise, significant crystallization of taxol would tend to stiffen the worm micelles, and also affect length distributions and degradation kinetics.

Initial distributions of FM-resolvable contour lengths (> 1 μm) of the worm micelles were plotted for ~200 worms (Fig. 1b). The histograms appear Gaussian with mean contour lengths of $\langle L \rangle \approx 15$ μm for OCL1 and $\langle L \rangle \approx 18$ μm for OCL3. With time, these giant OCL worm micelles spontaneously shorten to spherical micelles as seen in FM (Fig. 2a), and confirmed by both TEM (Supple. 1) and DLS (data not shown). Such a worm to sphere transition is driven by hydrolytic degradation of PCL by an 'end-cleavage' mechanism, which increases f_{EO} and consequently shifts the preferred morphology towards a higher curvature structure [23]. By the time OCL worms completely shorten to spherical micelles, GPC and NMR studies show that PCL chains have lost ~30% of their length by hydrolysis and f_{EO} correspondingly has increased from 0.42 to 0.55, which strongly favors spherical micelle formation, Scheme 1 [2,23]. The degradation-driven morphological change, i.e. contour length shortening of worm micelles to spherical micelles, can be conveniently visualized (Fig. 2a)

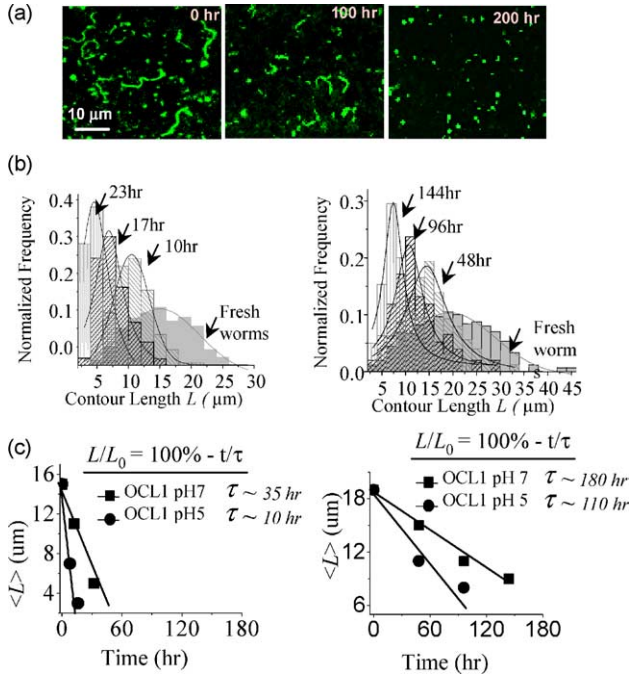

Fig. 2. Degradable OCL worm micelles spontaneously shorten in length with time and generate spherical micelles. (a) Visualization of the shortening by FM. (b) Contour length distribution shifting towards spherical micelles, fit by Gaussian or Lorentzian for ~200 worms. (c) Mean contour length (L) of OCL worm micelles decreases with time under physiological conditions, pH 5 Hepes and pH 7 PBS buffer, at 37 °C.

and quantitatively analyzed by FM. At different degradation times, contour length distributions of OCL worms were plotted for ~200 worms (Fig. 2b). The mean contour length $\langle L \rangle$ decreases gradually from the initial ~15–18 μm long worms towards spheres with time, and the distribution of contour length narrows as $\langle L \rangle$ shortens. It takes ~28 h for OCL1 and ~200 h for OCL3 worm micelles to completely transition into spherical micelles at 37 °C in water.

To study how OCL worm micelles degrade under physiological conditions, we used two different buffers, pH 7 PBS and pH 5 Hepes, to mimic the neutral-pH plasma and acidic intracellular endo/lysosome compartments, respectively. Since, PCL hydrolysis degradation is the rate-limiting step in OCL worm micelle shortening kinetics [23], degradation kinetics can be characterized by the corresponding shortening rate. The mean contour lengths $\langle L \rangle$ of OCL worm micelles at different times were obtained from contour length distribution

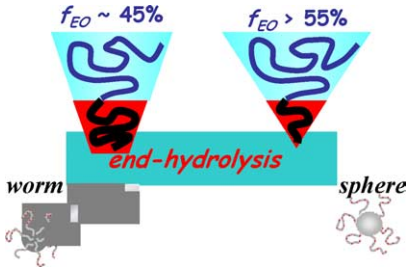

Scheme 1. Schematic illustration of end-hydrolysis of PCL leading to increase of f_{EO} and worm-to-sphere transition of PEO–PCL.

curves in each buffer solution at 37 °C and were plotted with time, Fig. 2c. For both buffers, the mean contour length $\langle L \rangle$ initially decays linearly with time and fits to $\langle L \rangle = \langle L \rangle_o(1 - t/\tau)$, where τ is the characteristic time. For OCL1, $\tau \approx 10$ h in pH 5 buffer and ≈ 35 h in pH 7 buffer, respectively, and for OCL3, $\tau \approx 110$ h in pH 5 buffer and ≈ 190 h in pH 7 buffer. At similar pH, the higher MW copolymer OCL3 worms shorten 5–10 fold slower than OCL1. At acidic pH 5, both copolymers shorten 2–3 fold faster than at neutral pH.

3.2. Evaluation of degradable OCL worm micelles for drug delivery

3.2.1. In vitro compatibility with blood and cultured cells

Incubating OCL worm micelles with whole blood for 2 days at 37 °C shows that they (i) do not adhere to red blood cells (RBC), (ii) remain suspended in the plasma, and (iii) retain their flexibility (Fig. 3a). Also, a hemolysis study of OCL worm micelles (10 mg/ml) shows negligible hemolytic activity (<1%), i.e. there is no interaction with these prototypical biomembranes, thus demonstrating hemocompatibility. In comparison, some low molecular weight surfactants currently used in intravenous administration, such as Tween 80, will readily lyse RBC [28].

Bovine aortic endothelial cells and vascular smooth muscle cells exposed to OCL worm micelles in PBS with a dose of 5 mg/ml showed no significant ill-effects for up to 5 days. Trypan blue exclusion tests showed 94±2 and 92±4% viability of endothelial cells after 1 day for untreated control cells and exposed cells, respectively (Fig. 3b). After 5 days, cell survival is still higher than 85% for exposed cells, compared to 89% for untreated control cells. Smooth muscle cells show similar viability results. Thus, OCL worm micelles

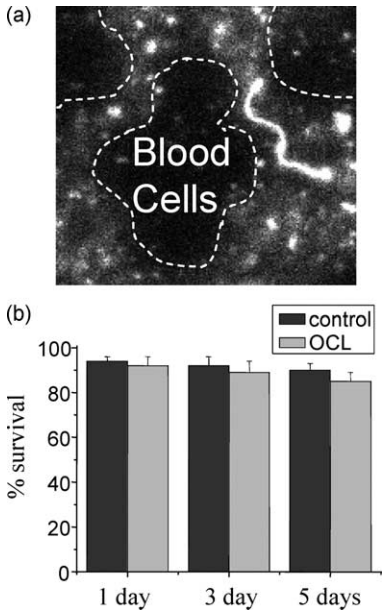

Fig. 3. In vitro compatibility with cultured cells and blood. (a) Incubation with whole blood. (b) Trypan blue assay on cytotoxicity of OCL worm micelles with bovine aortic endothelial cells (similar results on vascular smooth muscle cells).

and their degradation product, 6-hydroxycaproic acid, cause little or no cell death compared to untreated cells, demonstrating that they are non-toxic and compatible with cultured vascular cells.

The current clinical formulation of the anti-cancer drug Taxol is in a 50:50 mixture of Cremophore EL (polyoxylated castor oil) plus dehydrated ethanol, and must be diluted 5–20-fold with saline or dextrose solution before intravenous administration [31,32]. Such a formulation causes serious side effects such as hypersensitivity, neurotoxicity and nephrotoxicity [31,32]. Here, degradable OCL worm micelles prove to be compatible with cultured cells and blood, offering a potential advantage over conventional surfactant alternatives as carriers for taxol.

3.2.2. Taxol loading into OCL worm micelles

As with polymer-based spherical micelles [14,28,29,33], the hydrophobic micellar core of OCL worm micelles provides a compatible non-polar environment to solubilize hydrophobic species that are otherwise only sparingly soluble in water. Taxol is aromatic and ~25% oxygen by mass, but it is clearly hydrophobic with a very low water solubility of approximately 0.0001% (w/w) [34]. PCL has a similar oxygen content (~30% by mass), but lacks any aromatic groups. Various groups have loaded taxol into PCL microspheres [35] or films [36], and PEO–PCL diblock or triblock copolymer nanospheres [37] and micelles [38] for sustained release. Reported drug loads greater than 10% (w/w) are common, but only below 10% weight fraction, has it been documented (with films) that taxol and PCL mix as a single phase.

With the OCL worm micelles here, taxol also appears to spontaneously partition into the hydrophobic cores and at drug:PCL weight fractions close to ~5% (Scheme 2 and Table 1). These maximum loading ratios, determined by HPLC, do not change significantly with worm micelle concentration. Additionally, loading taxol into the worm micelles does not significantly change their flexibility or degradation kinetics (as assessed by FM per Fig. 1). As mentioned above, crystallization or swelling of the core would tend to stiffen the worm micelles. For example, a 20% increase in worm micelle diameter (such as with chain stretching to accommodate taxol) would lead to a 65% larger l_p, which would be very easily detected.

The net loading capacity of OCL worm micelles significantly enhances the solubility of taxol in water. Dilute solutions of 1 wt% OCL worm micelle in water can dissolve 0.3–0.5 mg taxol per milliliter, which is ~100 to 1000-fold higher than the solubility of free taxol in water. At 10–15 wt%

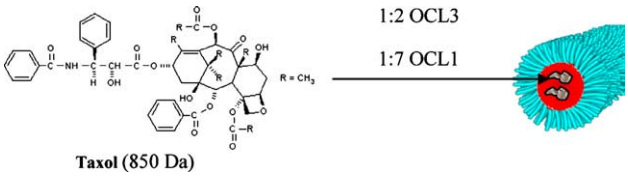

Scheme 2. Schematic illustration of physical encapsulation of taxol into the hydrophobic core of PEO–PCL worm micelles.

Table 1
Loading and burst loss of taxol from OCL worm micelles

	PCL M_n	Core diameter (nm)	Taxol loading (%w/w) (%)	pH 5 (%)	pH 7 (%)
OCL1	2700	11	4.5	~60	~50
OCL3	6400	29	6.7	~40	~30

OCL, solubilization increases to 3–7.5 mg taxol per milliliter, which is comparable to the maximum taxol solubility in clinically used formulations with Cremophore EL (6 mg/ml) [32].

The larger diameter OCL3 worm micelle does appear to load about 50% more drug than the smaller diameter OCL1 worm micelles (Table 1: 6.7 vs 4.5%, respectively). The CMCs of these polymer micelles are too low to explain any difference. Also, since the PCL surface area per mass of these particles is larger (by a factor 29/11 = 2.6, Table 1) for OCL1 than for OCL3, the higher loading for OCL3 rather than OCL1 does not seem consistent with interfacial adsorption. On the other hand, the larger relative loading is consistent with simple partitioning into the PCL cores, as expected from past reports.

Given the large size of the worm micelles, the taxol loads above are intriguing. They imply that if a single, 10 μm-long worm micelle (e.g. OCL1) carries its load of 10^4–10^5 molecules of taxol into a typical cell (of cell volume ~1 picoliter), then there is more than enough drug (concentration of ~100 nM) to kill the cell—since cytotoxic concentrations of taxol are ~10 nm [39]. Approximately, 1000 spherical micelles would be required to achieve the same toxic dose to a cell. However, with worm micelles, all of the drug can be delivered to the cell at once, would only be part of a larger statistical variation delivery by 1000 spherical micelles. Based on this estimation alone, drug resistant cells seem less likely to emerge with worm micelle delivery of taxol.

3.2.3. Storage of taxol loaded OCL worm micelles

OCL worm micelle degradation rate increases with temperature and acidic pH [23]. At 4 °C and in PBS (pH 7), taxol loaded OCL worm micelles remain stable with negligible degradation for weeks (for OCL1) or months (for OCL3). These would seem to be useful shelf-lifes for such formulations. Taxol loaded OCL worm micelles in pH 7 PBS solutions can thus be conveniently stored in a 4 °C refrigerator before administration.

3.2.4. In vitro release of taxol from OCL worm micelles

We used a dialysis method to mimic in vivo 'sink conditions' [11] and to study the release kinetics of taxol from OCL worm micelles. Fig. 4 shows the percentage of taxol released from OCL1 (a) and OCL3 (b) worm micelles versus time at 37 °C, in pH 5 Hepes and pH 7 PBS physiological buffers. After an initial burst release, typical for polymeric micelle systems [11,40], a much slower and sustained release was observed to completion for both OCL1 and OCL3. The initial burst release, i.e. 50–60% of taxol released from OCL1 within 1 h and 30–40% of taxol released from OCL3 within

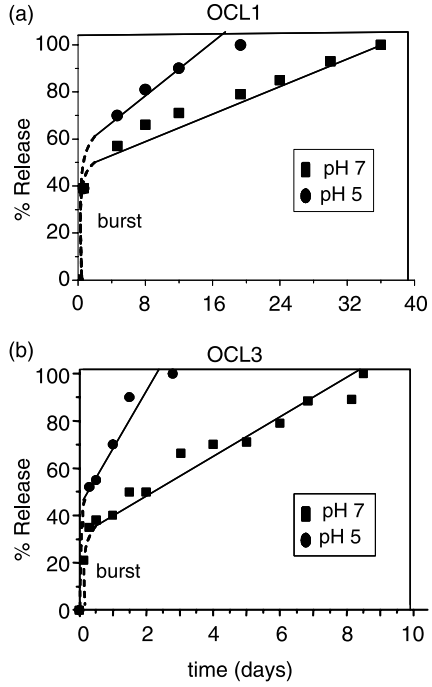

Fig. 4. Release profiles of taxol from (a). OCL1 worm micelles and (b). OCL3 worm micelles in pH 5 Hepes and pH 7 PBS buffers at 37 °C.

4 h, Table 1, perhaps reflects weak localization of some of the drug in the core–corona interface region. Such drug does not have to diffuse through the large segments of the core to exit the micelle, and so its release is rapid [11,39]. The percentage of burst release is about twice larger for OCL1 than OCL3, probably because OCL3 has a much larger PCL block and thus a hydrophobic core of larger diameter ($d=29$ nm) compared to OCL1 ($d=11$ nm) so that proportionately less taxol partitions to OCL3's core–corona interface.

After the fast initial burst of drug loss, the remaining taxol is released gradually (Fig. 4). For OCL1, taxol was released over a 10 h period at pH 5 and over 36 h at pH 7. For OCL3, taxol was released over a 3 day period at pH 5 and over 8 days at pH 7. As with the differences in burst release, such different taxol release times seem likely to reflect the underlying physicochemical processes that lead to faster OCL worm micelle degradation kinetics with decreasing pH [23]. Indeed, Fig. 5 shows the extremely slow and pH-independent release of

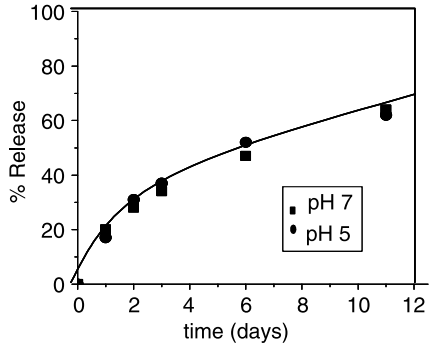

Fig. 5. Release profiles of taxol from OCL1 worm micelles in pH 5 Hepes and pH 7 PBS buffers at 4 °C.

Table 2
Worm micelle shortening and release of taxol

	Cross-sectional area (nm^2)	Shortening pH 5 (% per h)	Shortening pH 7 (% per h)	Release pH 5 (% per h)	Release pH 7 (% per h)
OCL1	121	3.8	2	3	1.5
OCL1 (4 °C)	121	–	–	0.14	0.14
OCL3	841	0.5	0.3	0.5	0.3

taxol from OCL1 worm micelles at 4 °C, where degradation is negligible [23].

Further comparison of taxol release rate with the corresponding OCL worm micelle degradation rate at 37 °C demonstrates that OCL worm micelle degradation dominates taxol release. The kinetics of taxol release is linear with time and the %/h release rates in Fig. 5a,b are tabulated in Table 2 together with the corresponding degradation-induced decay of mean contour length, $\langle L \rangle$, as a percent initial length with time (Fig. 2); this is also initially linear. The degradation/shortening rates, expressed as percentage of length change per hour, are essentially the same as the taxol release rate. Moreover, the release of taxol is complete when worm micelles are essentially gone but spherical micelles persist. These results imply a tight coupling between degradation and release.

3.3. A simple geometric model for degradation-coupled release

One possible contribution to consider for the coupling of the sustained drug release (after the initial burst) to the worm-to-sphere transition is that worm micelles carry more drugs than spherical micelles. This is expected because worms and spheres composed of the same copolymer will tend to have a similar area per copolymer due to the shared interfacial chemistry (i.e. a hydrated junction of PEO–PCL) and therefore common interfacial energy density (i.e. the interfacial tension, γ). However, worm micelles have a larger volume to surface area ratio. Defining $r=d/2$, a long cylinder has

$$(\text{Cylinder volume/Area}) = (\pi r^2 L/2\pi rL) = r/2$$

In comparison, for n spheres of the same radius and same total mass as a given worm,

$$(n \text{ Sphere volumes}/n \text{ Areas}) = (4/3\pi r^3 n/4\pi r^2 n) = r/3$$

Comparing the two ratios for micelles of the same radius yields

$$\text{Cylinder/Sphere} = 3r/2r = 1.5$$

This equates to 50% more drug carrying capacity in the worm micelle's core. Additionally, as OCL worm micelles break down to spherical micelles, PCL degradation progressively decreases the mass of the hydrophobic block and further reduces the drug carrying capacity of spherical micelles. Release of the drug during the transition from worm micelles to spheres is therefore understandable.

The degradation-dominated release behavior enables controlled drug release via tuning of degradation rate of OCL worm micelles. We have recently shown that blocking the

chain-end hydroxyl of the PCL dramatically delays hydrolytic degradation [23]. In addition, we show here that low pH fosters degradation-coupled release of the drug, which is especially interesting for delivery of anti-cancer drugs to tumor tissues. While most of the drug remains partitioned within OCL worm micelles that would show relatively slow release rate during circulation in blood (pH 7), faster release will occur once the micelles reach the tumor site where pH is lower than that in the normal tissue [15,41]. Furthermore, since polymeric micelles are usually internalized into the cells by endocytosis [42,43], the acidity of the endosome/lysosome should lead to accelerated drug release inside the cancer cells and faster a therapeutic effect.

4. Conclusion

We have visualized giant, flexible worm micelles self-assembled from degradable copolymer, PEO–PCL, by Fluorescence Video Microscopy, and we characterized their thermodynamic, degradation-induced morphological worm-to-sphere transition. Degradable PEO–PCL worm micelles prove to be compatible with cultured cells and blood, as well as capable of loading a model anti-cancer drug taxol into the hydrophobic core with convenient storage. Subsequent release of taxol is dominated by OCL worm micelle degradation, demonstrating significant potential as a novel controlled-release drug delivery vehicle.

Appendix. Supplementary Data

Supplementary data associated with this article can be found, in the online version, at 10.1016/j.polymer.2005.11.093

References

[1] Alexandridis P, Lindman B. Amphiphilic block copolymers: self-assembly and applications. New York: Elsevier; 2000.
[2] Jain S, Bates FS. Science 2003;300:460–4.
[3] Discher BM, Won YY, Ede DS, Lee JCM, Bates FS, Discher DE, et al. Science 1999;284:1143.
[4] Discher BM, Bermudez H, Hammer DA, Discher DE. J Phys Chem B 2002;106:2848–54.
[5] Ahmed F, Hategan A, Discher DE, Discher BM. Langmuir 2003;19:6505–11.
[6] Lee JCM, Santore M, Bates FS, Discher DE. Macromolecules 2002;35:323–6.
[7] Bermudez H, Aranda-Espinaza H, Hammer DA, Discher DE. Europhys Lett 2003;64:4–10.
[8] Hadjichristidis N, Pispas S, Floudas GA. Block copolymers: synthetic strategies, physical properties and application. New York: Wiley; 2003.
[9] Discher DE, Eisenberg A. Science 2000;297:967.
[10] Kataoka K, Harada A, Nagasaki Y. Adv Drug Deliv Rev 2001;47:113–31.
[11] Soo PL, Luo L, Maysinger D, Eisenberg A. Langmuir 2002;18:9996–10004.
[12] Piskin E, Denkbas EB, Kucukyavuz Z. J Biomater Sci Polym Ed 1995;7:359–73.
[13] Shin IG, Kim SY, Lee YM, Cho CS, Sung YK. J Control Release 1998;50:79–92.
[14] Soga O, van Nostrum CF, Fens M, Rijcken CJF, Schiffelers RM, Storm G, et al. J Control Release 2005;103:341–53.
[15] Shuai X, Ai H, Nasongkla N, Kim S, Gao J. J Control Release 2004;98:415–26.
[16] Klibanov AL, Maruyama K, Torchilin VP. FEBS Lett 1990;268:235–7.
[17] Photos PJ, Bacakova L, Discher BM, Bates FS, Discher DE. J Control Release 2003;90:323–34.
[18] Hubbell JA. Science 2003;300:595–6.
[19] Yokoyama M, Okano T, Sakurai Y, Ekimoto H, Shibazaki C, Kataoka K. Cancer Res 1991;51:3229–36.
[20] Dalhaimer P, Bates FS, Discher DE. Macromolecules 2003;36:6873–7.
[21] Kim YH, Dalhaimer P, Christian D, Discher DE. Nanotechnology 2005;16:S484–S91.
[22] Dalhaimer P, Geng Y, Photos P, Discher DE, In preparation.
[23] Geng Y, Discher DE. J Am Chem Soc 2005;(37):12780–1.
[24] Geng Y, Ahmed F, Bhasin N, Discher DE. J Phys Chem B 2005;109:3772–9.
[25] Won YY, Davis HT, Bates FS. Science 1999;283:960.
[26] Spencer CM, Faulds D. Drugs 1994;48:794.
[27] Luo L, Tam J, Maysinger D, Eisenberg A. Bioconjugate Chem 2002;13:1259–65.
[28] Lee SC, Kim IC, Kwon H, Chung SY. J Control Release 2003;89:437–46.
[29] Zhang C, Qineng P, Zhang H. Colloids Surf B: Biointerfaces 2004;39:69–75.
[30] Dalhaimer P, Bermudez H, Discher DE. J Polym Sci B 2003;42:168–76.
[31] Dorr RT. Ann Pharmacother 1994;28:S11.
[32] Gelderblom H, Verweij J, Nooter K, Spareboom A. Eur J Cancer 2001;37:1590–8.
[33] Burt HM, Zhang X, Toleikis P, Embree L, Hunter WL. Colloids Surf B: Biointerfaces 1999;16:161–71.
[34] Liggins RT, Hunter WL. J Pharm Sci 1997;86:1458.
[35] Dordunoo SK, Jackson JK, Arsenault LA, Oktaba AM, Hunter WL, Burt HM. Cancer Chemother Pharmacol 1995;(4):279–82.
[36] Shi R, Burt HM. Int J Pharm 2004;271(1-2):167–79.
[37] Kim SY, Lee YM. Biomaterials 2001;22(13):1697–704.
[38] Shuai X, Merdan T, Schaper AK, Xi F, Kissel T. Bioconjug Chem 2004;15(3):441–8.
[39] Torres K, Horwitz SB. Cancer Res 1998;58(16):3620–6.
[40] Teng Y, Morrison ME, Munk P, Webber SE, Prochazka K. Macromolecules 1998;31:3578–87.
[41] Hoes CJT, Boon PJ, Kaspersen F, Feijen J. Makromol Chem Macromol Symp 1993;70/71:119–36.
[42] Kakizawa Y, Kataoka K. Adv Drug Deliv Rev 2002;54:203–22.
[43] Savic R, Luo L, Eisenberg A, Maysinger D. Science 2003;300:615–8.